Copper-carboxamide complex immobilized on nano NaY zeolite: an efficient catalyst for xanthenes synthesis

Hamidreza Younesi[1] · Sakineh Asghari[1] · Ghasem Firouzzadeh Pasha[1] · Mahmood Tajbakhsh[1]

Abstract

This paper describes the direct synthesis of carboxamide-functionalized nano NaY zeolite (CBA-Ze) to develop a new high-functionality nanocatalyst in one pot process. This surface functionalization was achieved using a four-component Ugi reaction. Afterward, copper ions were coordinated with Ugi-ligands decorated on the nano NaY zeolite surface. To characterize the synthesized catalysts, fourier transform-infrared spectroscopy (FT-IR), thermogravimetric analysis (TGA), differential thermal analysis, scanning electron micrograph, transmission electron microscopy, X-ray diffraction (XRD), dynamic light scattering, energy dispersive spectroscopy, inductively coupled plasma, and elemental analyses were used. The nature of the supported Ugi-ligand on the zeolite's surface improved the catalyst reactivity of the zeolite, made it more homogeneous, and increased its ability to coordinate with copper ions. The catalytic activity of the synthesized copper-carboxamide complex immobilized on nano NaY zeolite (Cu@CBA-Ze) was investigated in the synthesis of Xanthen derivatives, resulting in product yields of 85–98% Cu@CBA-Ze using only 20 mg in H_2O:EtOH (1:1) at room temperature within 30 min. In addition to the ease of recovering and reusing catalyst, and the simple setup procedure, this method is an eco-friendly, benign procedure for synthesizing heterocycles. This study describes a catalytic system with the potential to produce other useful heterocyclic compounds under mild environmental conditions.
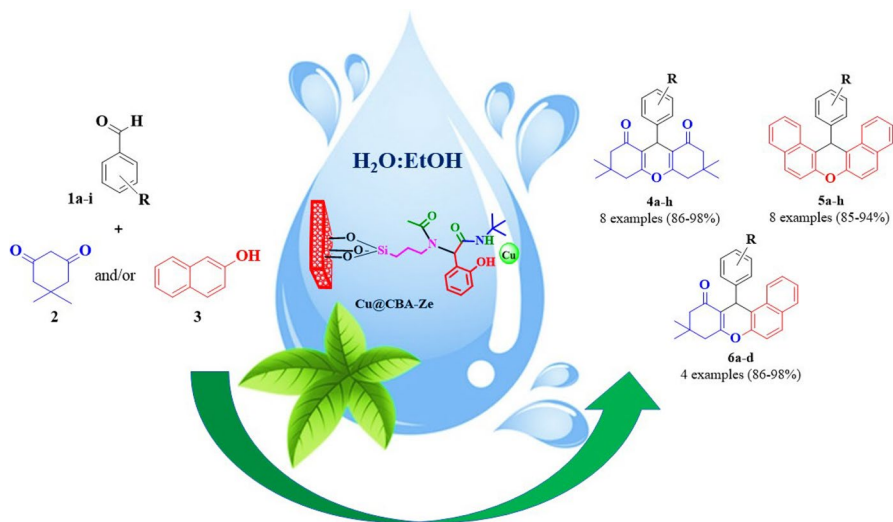
✉ Sakineh Asghari
s.asghari@umz.ac.ir

✉ Ghasem Firouzzadeh Pasha
ghasemf.pasha@umail.umz.ac.ir; ghasempasha@yahoo.com

Hamidreza Younesi
hr.younesi1@gmail.com

Mahmood Tajbakhsh
tajbaksh@umz.ac.ir

1   Department of Organic Chemistry, Faculty of Chemistry, University of Mazandaran, Babolsar 47416-95447, Iran

Graphical abstract

Introduction

Nanomaterials are used to immobilize homogeneous catalysts and enhance their catalytic reactivity, efficiency, and stability. Various nanomaterials are available, including nanozeolites, which have high specific surfaces, are non-toxic, and can be reused [1]. With the increasing use of functionalized nano-zeolites for the synthesis of organic chemicals such as chromens [2, 3], pyrrols [4], and pyrimidines [5], the modification of nano-zeolites has gained increasing attention.

In recent years, multicomponent approaches as well as materials chemistry have been combined to create new functional materials. They result in lower costs, lower waste, and reduced pollution by reducing complexity and substrate variety. In addition, they reduce the number of atoms, pots, and steps [6]. It is well known that Ugi's four-component reactions (Ugi-4CRs) produce a high level of molecular complexity when performed in one pot due to the intimate nature of their reactions. As a result, atomic economy, bond numbers, and stereochemical diversity were high [7, 8]. It produces complex pseudo peptides with carboxamide functionality by a Ugi four-component reaction [9–11]. In coordination chemistry and catalysts for hydrogen bonding, carboxamides [–C(O)NH–] play a crucial role, as well as being crucial protein building blocks [12]. Recent research has used Ugi-4CR as a catalyst for producing pyrrols [4] and a new kind of carbonaceous-based drug carrier [13, 14].

Xanthenes are an important class of heterocyclic compounds with various applications such as dyes [15], lasers [16], and pH-sensitive fluorescent materials for the visualization of biomolecules [17], as well as possessing pharmaceutical and biological properties like anticancer [18], antiviral [19], analgesic and antibacterial [20], anti-inflammatory [21], antimalarial [22], anticonvulsant [23], antimicrobial [24], antiplatelet [25], antigenotoxic [26], antiphlogistic [27], and antifungal activities [28, 29].

Due to these properties, extensive research was conducted on xanthenes synthesized with different catalysts, including silica sulfuric acid [30], Fe@Zeolite [31], I_2 [32], core/shell Fe_3O_4@GA@isinglass [33], Fe_3O_4@PS@His [HSO^{4-}] [34], Cu (II)-Fur-APTES/GO [35], perlite NPs@IL/ZrCl$_4$ [36], Cobalt (II) complex [37], Fe_3O_4@SiO_2-TEA-HPA [38], $NiCuFe_2O_4$ [39], (TTTMS) [40], p-sulfonic acid calix [4] arene [41], [MIMPS][HSO$_4$] [42], [DMEA][HSO$_4$] [43], and Cux-Cr100-x–MOF [44].

Although these catalysts offer some improvement, many of them suffer from some disadvantages, such as long reaction times [30, 32, 38], harsh reaction conditions [30, 40, 42, 43], toxic solvents [30], and low reaction yields [30, 33]. Therefore, there is a need to develop a simple, cost-effective, energy-efficient, and environmentally friendly catalytic system for xanthene synthesis. However, recovering and reusing nanocatalysts has been staying a significant challenge. A possible solution to this issue involves using heterogeneous nanocatalysts due to their distinct properties including, simplicity of catalyst separation, high stability, eco-friendliness, low cost, easy availability, and less corrosivity. Therefore, there is considerable attention to designing and synthesizing new heterogeneous catalytic systems to address these problems.

The application and preparation of functionalized nanozeolites are currently of interest to us [2–5]. In this paper, we present a multicomponent ligation approach using Ugi-four components for the chemical attachment of carboxamide ligands on the surface of nano NaY zeolite (CBA-Ze). In turn, this led to the development of novel nanocatalysts that were highly compatible with copper ions (Cu@CBA-Ze). In this study, a recyclable and eco-friendly nanocatalyst (Cu@CBA-Ze) was found to be applied to the preparation of xanthene derivatives.

Results and discussion

In order to achieve homogenized nano NaY zeolite, (3-aminopropyl)triethoxysilane (APTES) was used, followed by 2-hydroxybenzaldehyde, tert-butylisocyanide, and acetic acid through a multicomponent reaction, which immobilized carboxamide functionality in grafted ligands, improving NaY zeolite dispersibility and reactivity. In nano NaY zeolite, Ugi-ligands were decorated with copper ions.

To prepare Ugi-four component functionalized nano NaY zeolite (CBA-Ze), nano NaY zeolite (Ze) was treated with APTES to produce silane-bonded nanozeolite (AP-Ze). As a result of a four-component reaction, 2-hydroxybenzaldehyde, tert-butylisocyanide, and acetic acid (AcOH) were combined with (AP-Ze) to yield the Ugi-modified nanocatalyst (CBA-Ze). As a next step, copper ions were immobilized
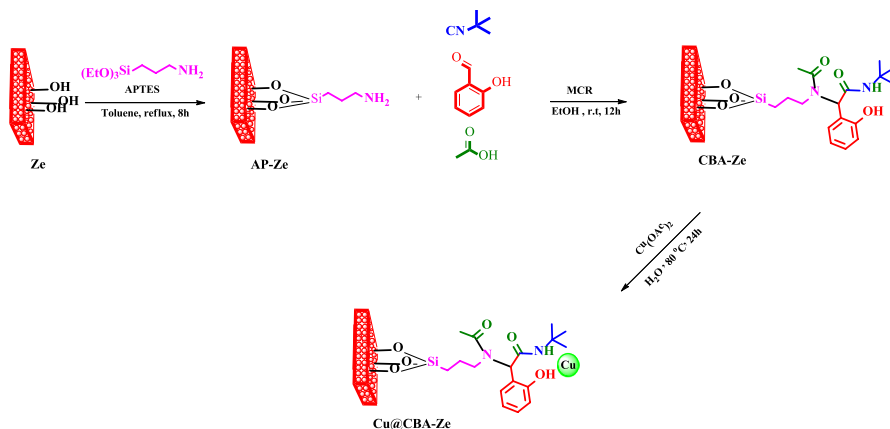
Scheme 1 Synthesis of the Cu@CBA-Ze

on the coating of carboxamide on the nano NaY zeolite (Cu@CBA-Ze). Because 2-hydroxybenzaldehyde has ligand-active –OH groups, we found that it is an appropriate bidentate ligand for metal chelates. An array of spectral techniques was used to characterize the samples' structures (Scheme 1), including FTIR, XRD, TGA, DTA, EDS mapping, DLS, SEM, TEM, elemental analyses, and ICP-OES.

FT-IR analysis

In Fig. 1, the FT-IR spectra of all synthesized samples are depicted. All common bands at 1100–1000 cm^{-1} (Si–O stretching), 1633 cm^{-1} (O–H bending), and 3500–3300 cm^{-1} (O–H stretching) vibrations can be seen in the FT-IR spectra of Ze, AP-Ze, CBA-Ze, and Cu@CBA-Ze, which exhibit all distinct bands [2, 5]. In the spectrum of AP-Ze, the appearance of vibrational bands at around 3205–3150 cm^{-1} (N–H stretching vibrations), 2932 cm^{-1} (C–H stretching vibrations), and 1460 cm^{-1} (C–H bending vibrations) confirm APTES is successfully attached to Ze's surface [45].

Infrared absorption bands at 3321 cm^{-1} (N–H stretching vibrations), 2965 cm^{-1} (C–H stretching vibrations), 1633 cm^{-1} (C=O stretching vibrations), and 1489 cm^{-1} (C–H bending vibrations) are depicted in the infrared spectrum of the Ugi product resulting from a one-pot pseudo-four component reaction between 2-hydroxybenzaldehyde, APTES, tert-butyl isocyanide, and AcOH. The infrared spectrum of CBA-Ze displays vibration bands at 3320 cm^{-1} related to (N–H stretching vibrations), 2927 cm^{-1} related to (C–H stretching vibrations), 1686 cm^{-1} (C=O stretching vibrations), 1489 cm^{-1} (C–H bending vibrations) and 1100 cm^{-1} (Si–O–Si absorption band), confirming the prosperous modification of the AP-Ze's surface through the Ugi-multicomponent reaction. The infrared spectrum of Cu@CBA-Ze exhibits vibration signals at 3321 cm^{-1} ascribed to (N–H stretching vibrations), 2929 cm^{-1} related to (C–H stretching vibrations), 1686 cm^{-1} (C=O stretching vibrations),

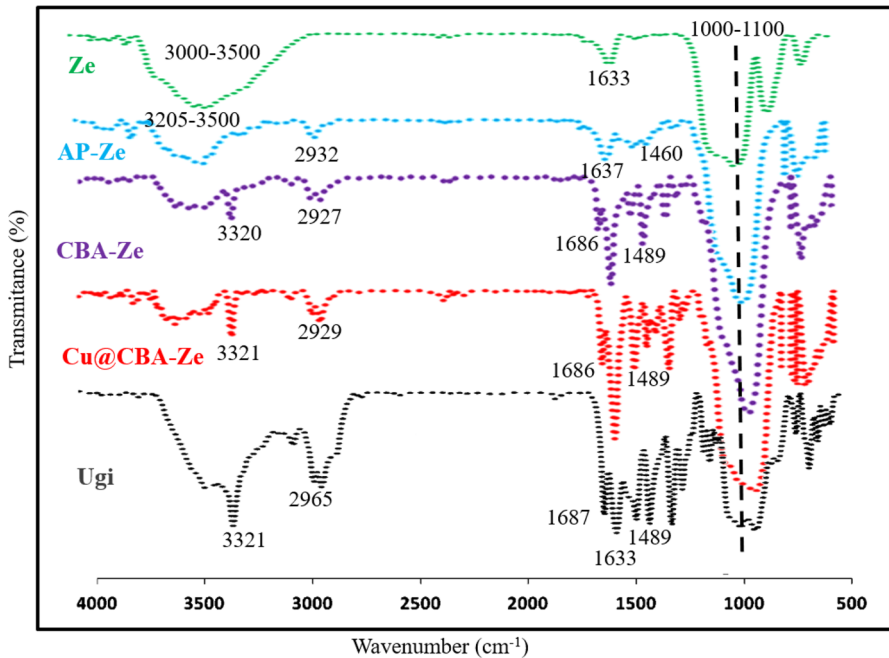**Fig. 1** Infrared spectra of Ze, AP-Ze, CBA-Ze, and Cu@CBA-Ze

1489 cm^{-1} (C–H bending vibrations) and 1100 cm^{-1} (Si–O–Si absorption band) [6, 46].

TGA analysis

The obtained data from TGA and DTA of Ze, AP-Ze, CBA-Ze, and Cu@CBA-Ze in the range of 30 and 600 °C at a rate of 10 °C/min are shown in Figs. 2 and 3, respectively. The TGA of Ze displays a weight loss at temperatures < 200 °C ascribed to the removal of physically adsorbed water molecules. The TGA diagram of AP-Ze exhibits a weight loss at temperatures < 150 °C related to physically adsorbed water molecules (12%) and a reduction between 300 and 450 °C for the removal of the organic moiety (aminopropyl group, 15%, 2.58 mmol/g).

The CBA-Ze's TGA profile shows two weight losses, at 120 °C attributed to the removal of the physically adsorbed water molecules (9%) and at 250–400 °C related to the organic moiety ((CH$_2$)$_3$N(CH$_3$CO) (CH(C$_6$H$_5$OH) (CONHC(CH$_3$)$_3$), 41%, 1.34 mmol/g. According to our results, the aminopropyl groups on AP-Ze are approximately 2.58, and the organic moiety on CBA-Ze is about 1.34 mmol/g. TGA data indicates that copper (II) oxide is present in the structure of Cu@CBA-Ze which results in higher char yields. Table 1 also shows the CHN analysis of AP-Ze and CBA-Ze, which indicates that CBA-Ze has a higher carbon content and contains nitrogen atoms than AP-Ze, indicating that AP-Ze was successfully perfumed
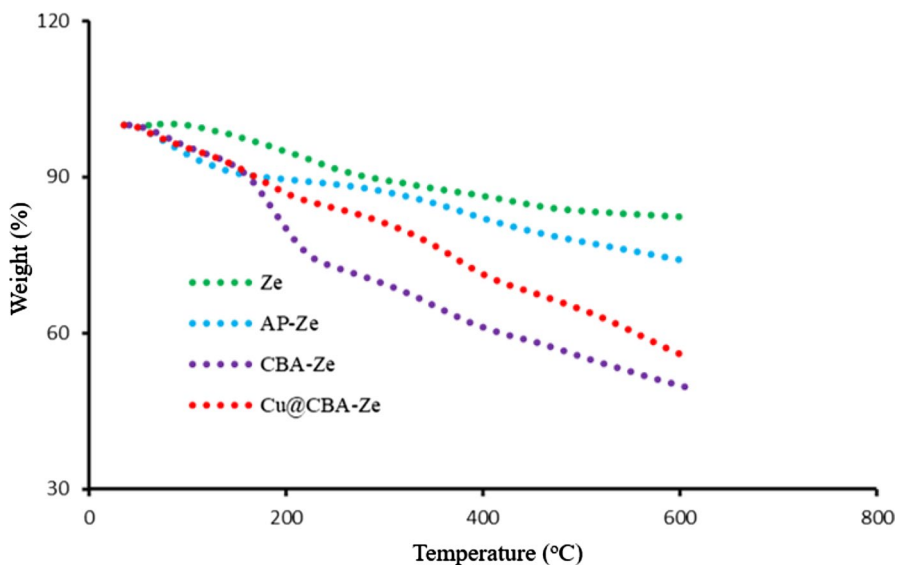
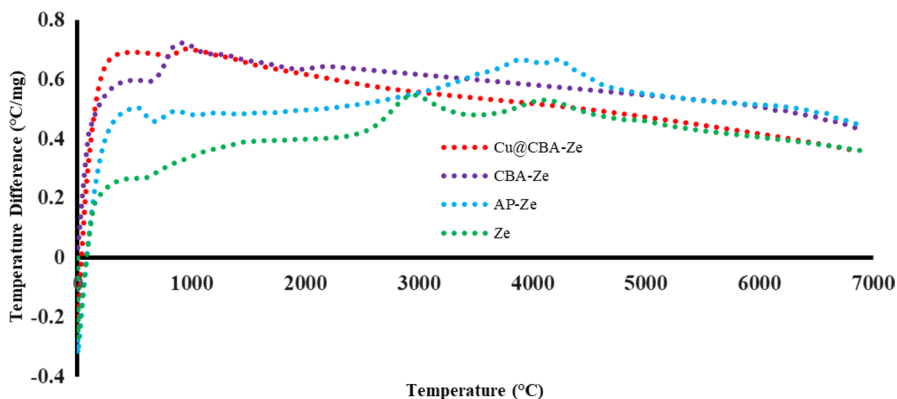**Fig. 2** TGA thermograms of Ze, AP-Ze, CBA-Ze and Cu@CBA-Ze

Fig. 3 DTA curves for Ze, AP-Ze, CBA-Ze, and Cu@CBA-Ze

Table 1 An analysis of CHN results for the AP-Ze and CBA-Ze products

Entry	Catalyst	C (wt %)	N (wt %)
1	AP-Ze	8.94	3.46
2	CBA-Ze	28.15	3.84

by the Ugi-multicomponent reaction. In agreement with the TGA data, the amount of Ugi product attached was 1.31 mmol/g. ICP analysis measured a copper load of 2.76 mmol/g on the surface of the CBA-Ze.

Morphological characteristics

The morphology of the synthesized catalysts was investigated using SEM images. As shown in Fig. 4, the SEM images of Ze, AP-Ze, CBA-Ze, and Cu@CBA-Ze are similar, indicating that modification on the NaY nanozeolite surface did not significantly change the morphology of nano NaY. The average particle sizes were ~ 40 to 80 nm.

Furthermore, TEM analysis was used for the structural characterization of the prepared catalysts. As illustrated in Fig. 5A, the TEM images of all samples indicate the mean particle size in the range of 80–100 nm which is in good agreement with SEM results. Also, a histogram of the diameter distribution of Cu@CBA-Ze is
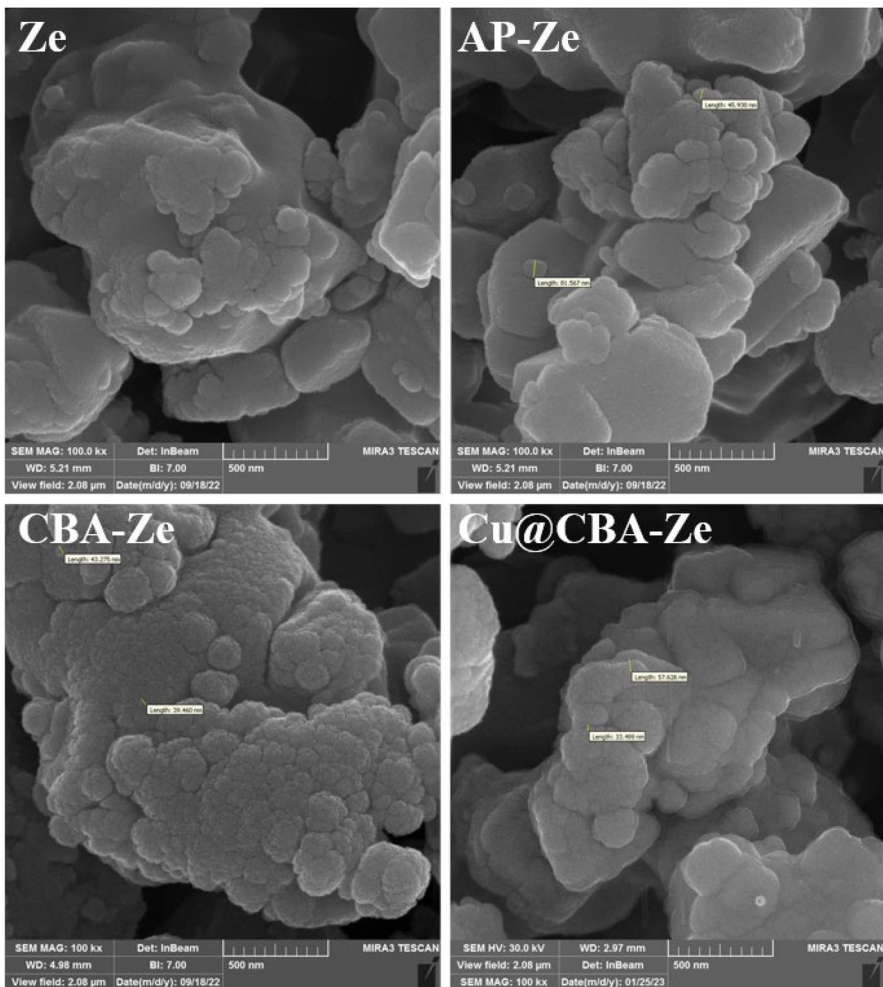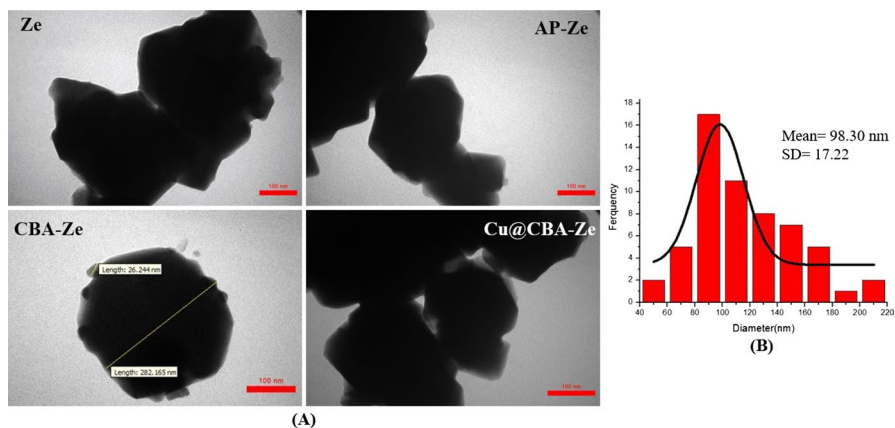

**Fig. 4** SEM images of Ze, AP-Ze, CBA-Ze, and Cu@CBA-Ze

Fig. 5 **A** The TEM images of Ze, AP-Ze, CBA-Ze, and Cu@CBA-Ze, and (**B**) size histogram patterns of Cu@CBA-Ze

displayed in Fig. 5B revealing the average particle size was approximately 98 nm, exhibiting slightly different from the obtained results from SEM results.

The elemental mappings of AP-Ze, CBA-Ze, and Cu@CBA-Ze are shown in Figs. 6, 7, and 8. The results display that Al, Si, O, C, N, and Cu were uniformly distributed throughout the catalyst surface which resulted in a uniform catalyst surface modification.
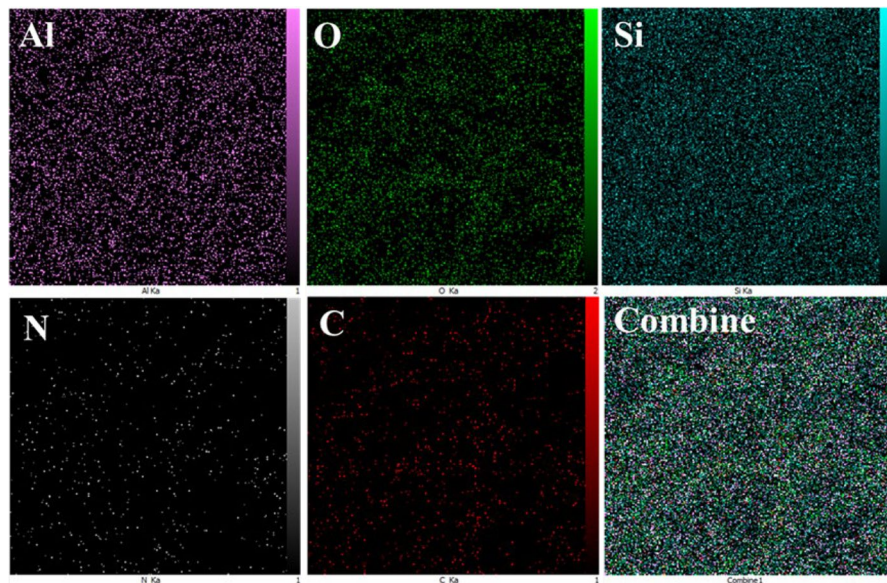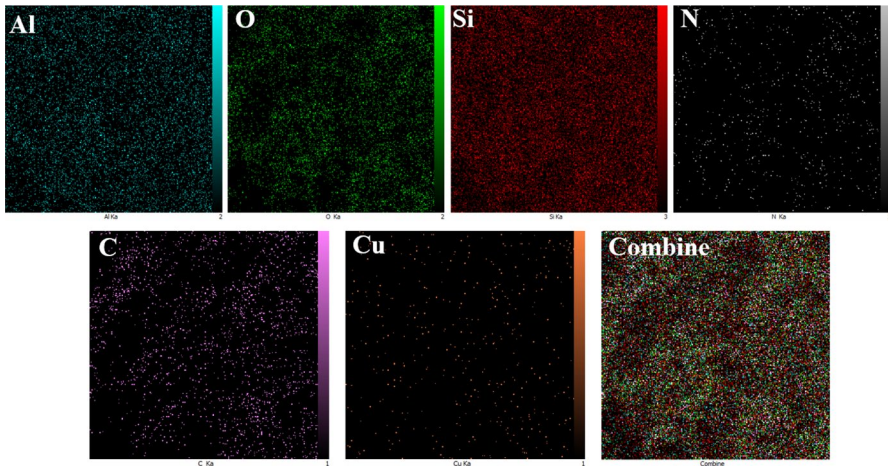

Fig. 6 Elemental mapping of the AP-Ze catalyst
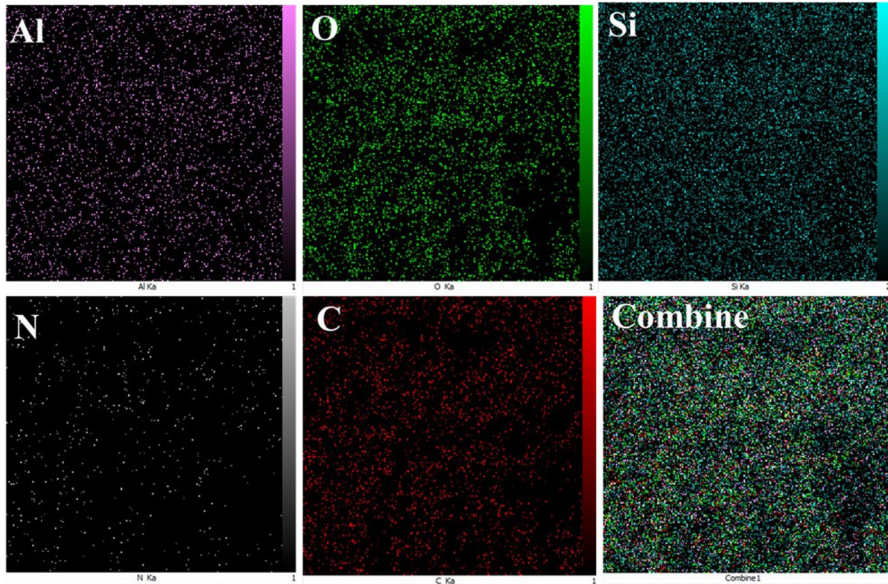
Fig. 7 Elemental mapping of the CBA-Ze catalyst

Fig. 8 Elemental mapping of the Cu@CBA-Ze catalyst

To determine the sizes and distributions of particles present in the liquid phase, the DLS analysis was provided based on the intensity of light scattered. Figure 9 shows an average particle size of 121 nm based on DLS analysis of Cu@CBA-Ze indicating a narrow particle size distribution. It was found that DLS results matched XRD, TEM, and SEM data well.
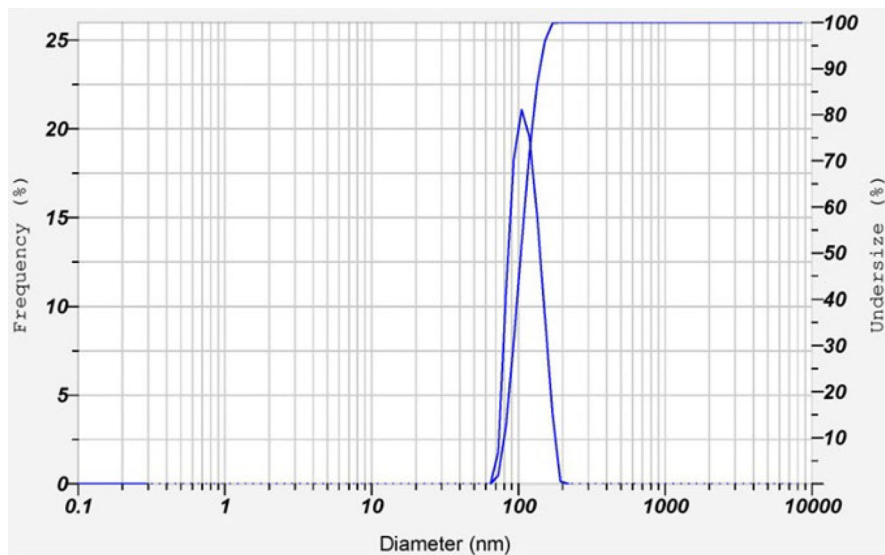
Fig. 9 DLS diagram of Cu@CBA-Ze catalyst

XRD analysis

As demonstrated in Fig. 10, Ze, AP-Ze, CBA-Ze, and Cu@CBA-Ze crystal structures were identified by applying X-ray diffraction patterns. It was found that all synthesized samples showed basic NaY zeolite reflection peaks in their XRD patterns confirming no significant changes in the nano NaY zeolite structure were observed after APTES and Ugi reactions, as confirmed by SEM analysis. Appearing of the peaks at 2θ: 36.51° and 42.52° ascribed to the Cu_2O phase indicating copper ions are successfully immobilized on the CBA-Ze's surface [47–49]. Based on the Debye Scherrer equation, the crystal sizes for Ze, AP-Ze, CBA-Ze, and Cu@CBA-Ze were 19.27, 21.54, 28.74, and 18.72 nm, respectively.

The activity of the Carboxamide-modified nano NaY zeolite immobilized with copper (Cu@CBA-Ze) has been examined for a three component reaction with aromatic aldehydes **1**, dimedone **2**, or β-naphthol **3** in the presence of a catalytic amount of Cu@CBA-Ze (Scheme 2).

The reaction of 4-chlorobenzaldehyde (1 mmol), and dimedone (2 mmol) in EtOH (10 mL) in the presence of a catalyst was chosen as a model reaction to achieve the optimal reaction conditions. This reaction was studied in the presence of several heterogeneous catalysts (Ze, AP-Ze, CBA-Ze, and Cu@CBA-Ze). Moreover, a catalyst-free reaction conditions were also tested (entry 1). In Table 2, Carboxamide-Functionalized nano NaY zeolite Immobilized with Copper (Cu@CBA-Ze) is shown to be an effective catalyst for the model reaction (entries 5, 8–22). The Ze, AP-Ze, CBA-Ze, Cu (OAc)$_2$, and Cu@CBA catalysts produced only traces of the product (entries 2–4 and 6, 7). Different amounts of Cu@CBA-Ze (10, 15, 20, 25, and 30 mg) (entries 5 and 8–11) were used for this reaction. Results indicate
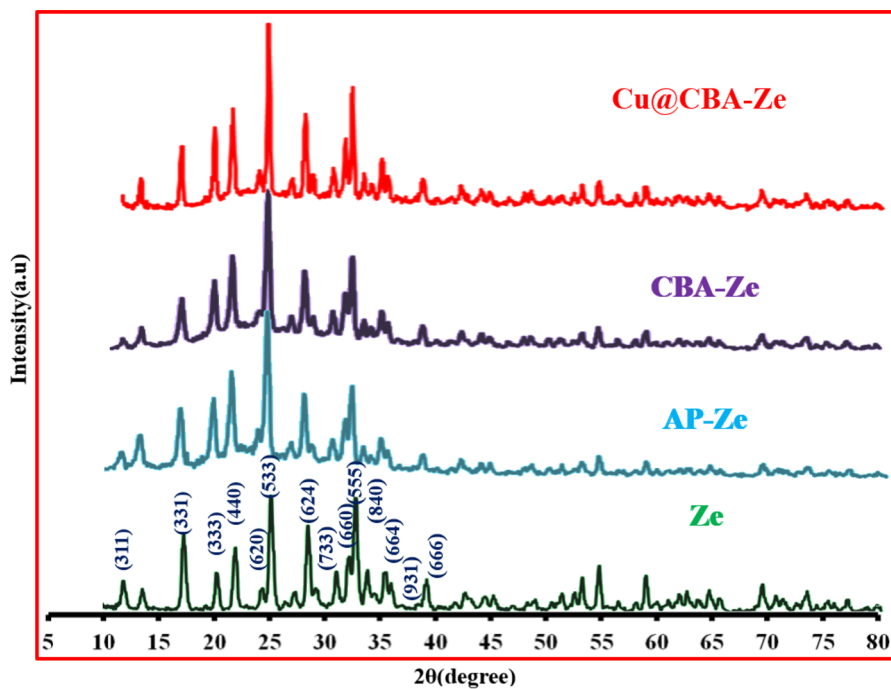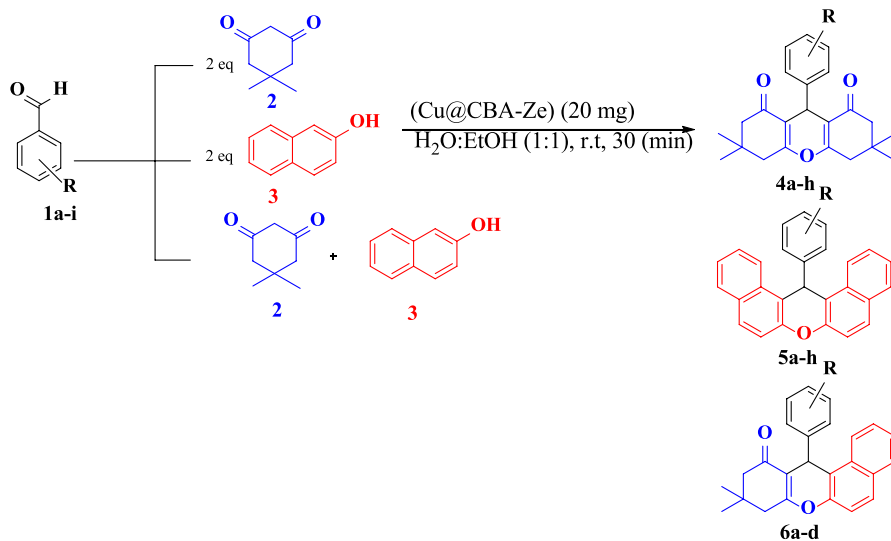
Fig. 10 XRD patterns of the Ze, AP-Ze, CBA-Ze, and Cu@CBA-Ze

Scheme 2 Synthesis of Xanthenes using Cu@CBA-Ze

Table 2 Optimization of reaction conditions for the synthesis of compounds **4b**

Entry	Catalyst (mg)	Solvent	Temperature °C	Time (min)	Yield %[a]
1	–	EtOH	r.t	240	Trace
2	Ze (10)	EtOH	r.t	240	Trace
3	AP-Ze (10)	EtOH	r.t	240	Trace
4	CBA-Ze (10)	EtOH	r.t	60	53
5	Cu@CBA-Ze (10)	EtOH	r.t	30	73
6	Cu (OAc)$_2$ (10)	EtOH	r.t	30	42
7	Cu@CBA (10)	EtOH	r.t	30	77
8	Cu@CBA-Ze (15)	EtOH	r.t	30	82
9	Cu@CBA-Ze (20)	EtOH	r.t	30	87
10	Cu@CBA-Ze (25)	EtOH	r.t	30	87
11	Cu@CBA-Ze (30)	EtOH	r.t	30	88
12	Cu@CBA-Ze (20)	H$_2$O	r.t	30	62
13	**Cu@CBA-Ze (20)**	**H$_2$O:EtOH (1:1)**	**r.t**	**30**	**98**
14	Cu@CBA-Ze (20)	MeOH	r.t	30	74
15	Cu@CBA-Ze (20)	CH$_3$CN	r.t	30	72
16	Cu@CBA-Ze (20)	DMF	r.t	30	81
17	Cu@CBA-Ze (20)	DMSO	r.t	30	84
18	Cu@CBA-Ze (20)	CH$_2$Cl$_2$	r.t	30	52
19	Cu@CBA-Ze (20)	Et$_2$O	r.t	30	47
20	Cu@CBA-Ze (20)	n-Hexane	r.t	30	42
21	Cu@CBA-Ze (20)	H$_2$O:EtOH (1:1)	40	30	98
22	Cu@CBA-Ze (20)	H$_2$O:EtOH (1:1)	78	30	98

Bold values related to the optimal condition which is described in the text

Reaction condition: 4-chlorobenzaldehyde (1 mmol), dimedone (2 mmol), in the presence of the catalyst in a solvent (10 ml)

[a]Isolated yields

that Cu@CBA-Ze is 20 mg in the optimized condition (entry 9). There was no improvement in reaction yield when catalyst amounts were increased (entries 10, 11). A range of solvents was then employed to test this model reaction, including H$_2$O, H$_2$O: EtOH (1:1), MeOH, CH$_3$CN, DMF, DMSO, CH$_2$Cl$_2$, Et$_2$O, and n-Hexane (entry 9 and 12–20). Reaction yields (entries 21 and 22) were not significantly increased by increasing the reaction temperature to 40 and 78 °C. According to Table 2, the model reaction performs well in the presence of Cu@CBA-Ze in H$_2$O: EtOH (1:1) at room temperature (entry 13).

As an extension of the scope of this reaction, different aromatic aldehydes (**1a–i**) were treated with dimedone (**2**) and/or β-naphthol (**3**) to extend the range of applications (Table 3). After determination of optimum conditions, the performance of the Cu@CBA-Ze as a catalyst for the synthesis of other xanthene derivatives was evaluated by the reaction of aromatic aldehydes and dimedone or β-naphthol. In all studied cases, Cu@CBA-Ze gave the corresponding products **4a–h**, **5a–h**, and **6a–d** in

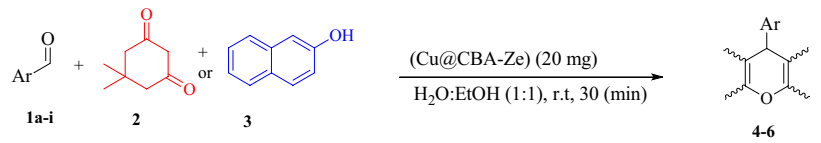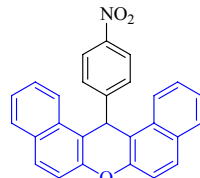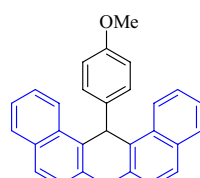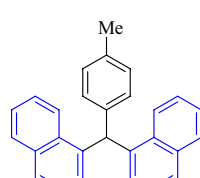**Table 3** Synthesis Xanthenes using Cu@CBA-Ze[a]
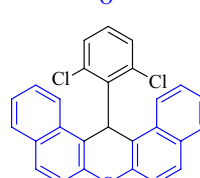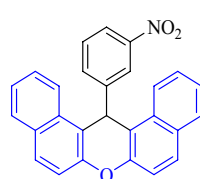
Entry	Product	Ar	Structure	MP °C [Ref]	Yield %[a]
1	**4a**	C_6H_5		204–205 [50]	94
2	**4b**	$4\text{-Cl-}C_6H_4$		233–235 [50]	98
3	**4c**	$4\text{-CN-}C_6H_4$		215–216 [51]	86
4	**4d**	$4\text{-NO}_2\text{-}C_6H_4$		230–232 [50]	97
5	**4e**	$4\text{-OMe-}C_6H_4$		252–253 [50]	92

Table 3 (continued)

Entry	Product	Ar	Structure	MP °C [Ref]	Yield %[a]
6	**4f**	4-Me-C$_6$H$_4$		229–230 [42]	89
7	**4 g**	3-NO$_2$-C$_6$H$_4$		166–168 [50]	91
8	**4 h**	3-Br-C$_6$H$_4$		286–287 [50]	93
9	**5a**	C$_6$H$_5$		182–184 [50]	91
10	**5b**	4-Cl-C$_6$H$_4$		284–285 [50]	92
11	**5c**	4-CN-C$_6$H$_4$		290–292 [52]	93

Table 3 (continued)

Entry	Product	Ar	Structure	MP °C [Ref]	Yield %[a]
12	**5d**	4-NO$_2$-C$_6$H$_4$		316–318[50]	94
13	**5e**	4-OMe-C$_6$H$_4$		202–204 [50]	85
14	**5f**	4-Me-C$_6$H$_4$		220–221 [53]	88
15	**5 g**	2,6-diCl-C$_6$H$_3$		274–276 [54]	92
16	**5 h**	3-NO$_2$-C$_6$H$_4$		215–216 [50]	88

Table 3 (continued)

Entry	Product	Ar	Structure	MP °C [Ref]	Yield %[a]
17	**6a**	4-Cl-C$_6$H$_4$		176–177 [50]	94
18	**6b**	4-CN-C$_6$H$_4$		199–201 [55]	95
19	**6c**	4-NO$_2$-C$_6$H$_4$		173–174 [50]	98
20	**6d**	3-Br-C$_6$H$_4$		160–161[50]	86

Reaction condition: aldehydes (1 mmol), dimedone (2 mmol), or β-naphthol (2 mmol), in the presence of the Cu@CBA-Ze (20 mg) in an H$_2$O: EtOH (10 ml, 1:1)

[a]Isolated yield

better yields, and shorter times in comparison to previously reported. The selectivity of the reaction was investigated in a competitive reaction between an equimolecular mixture of dimedone and β-naphthol with benzaldehyde derivatives in the presence of the Cu@CBA-Ze under the same reaction conditions (entries 17–20). The outcomes revealed that only asymmetric products **6a–d** were obtained in excellent yields. This is might be due to the faster reaction rate of aldehyde with dimedone

rather than with β-naphthol leading to the formation of knovenagle adduct, which then reacts with β-naphthol in the absence of dimedone resulting in asymmetric products **6a–d**. This assumption was verified with TLC monitoring of the three-component reaction of 4-nitrobenzaldehyde, dimedone, and β-naphthol (see S1-2). To confirm the structures of synthesized Xanthenes, we compared their physical properties and ^1H and ^{13}C NMR spectra to published data.

The results obtained by using the present catalytic approach for the synthesis of xanthenes were compared with those published previously to demonstrate the efficacy of the method (Table 4). Applying different catalysts such as Zr (DP)$_2$ (entry 1), SBSSA (entry 2), Fe^{3+}-montmorillonite (entry 3), ZnO–CH$_3$COCl (entry 4), CaCl$_2$ (entry 5), [bmim]HSO$_4$ (entry 6), p-sulfonic acid calix 4] arene (entry 7), boric acid (entry 8), CuO NPs (entry 9), Fe$_3$O$_4$@PS@His (entry 10), Cu (II)-Fur-APTES/GO (entry 11), perlite NPs@IL/ZrCl$_4$ (entry 12), and [cmmim][BF4] (entry 13), The xanthenes were obtained in lower yields (83–98%) and longer reaction times. Nevertheless, the catalyst system introduced led to the reaction proceeding at 25 °C in H$_2$O: EtOH (1:1) and producing the desired product whit 98% yield after 30 min (entry 14). Based on these results, we can conclude that Cu@CBA-Ze nanocatalyst may be an excellent alternative catalyst for preparing xanthenes.

Cu@CBA-Ze catalyzes the synthesis of xanthene derivatives by activating the carbonyl group of aldehydes making it more susceptible to nucleophilic attack by dimedone to form intermediate (I), followed by Michael's addition of another molecule of dimedone to form the intermediate (II). Intramolecular cyclization occurs after successive elimination of H$_2$O which results in the desired product and regenerates Cu@CBA-Ze in the reaction mixture (Scheme 3).

Table 4 Catalytic activity comparison of Cu@CBA-Ze with literature-reported catalysts in the synthesis of **4b**

| Entry	Catalyst (amount)	Conditions	Time	Yield (%) [Ref]
1	Zr (DP)$_2$ (60 mg)	EtOH/reflux	24 h	98 [56]
2	SBSSA (30 mg)	EtOH/reflux	10 h	98 [57]
3	Fe^{3+}-montmorillonite (80 mg)	EtOH/100 °C	6 h	88 [58]
4	ZnO–CH$_3$COCl (48 mg)	CH$_3$CN/reflux	5 h	90 [59]
5	CaCl$_2$ (17 mg)	DMSO/85–90 °C	4 h	83 [60]
6	[bmim]HSO$_4$ (100 mg)	solvent free/80 °C	3 h	95 [61]
7	p-sulfonic acid calix [4] arene (12 mg)	EtOH/80 °C	35 min	95 [41]
8	boric acid (3 mg)	solvent free/120 °C	20 min	96 [62]
9	CuO NPs (7 mg)	solvent-free/100 °C	14 min	90 [63]
10	Fe$_3$O$_4$@PS@His [HSO$_4^-$] (80 mg)	EtOH/reflux	10 min	96 [34]
11	Cu (II)-Fur-APTES/GO (20 mg)	EtOH: H$_2$O/50 °C	30 min	92 [35]
12	perlite NPs@IL/ZrCl$_4$ (5 mg)	solvent free/80 °C	120 min	88 [36]
13	[cmmim][BF4] (200 mg)	microwave irradiation/r.t	1 h	94 [64]
14	**Cu@CBA-Ze (20 mg)**	**H$_2$O: EtOH (1:1)/r.t**	**30 min**	**98[a]**

Bold values related to this work which is provided in the form of a table footnote

[a]This work
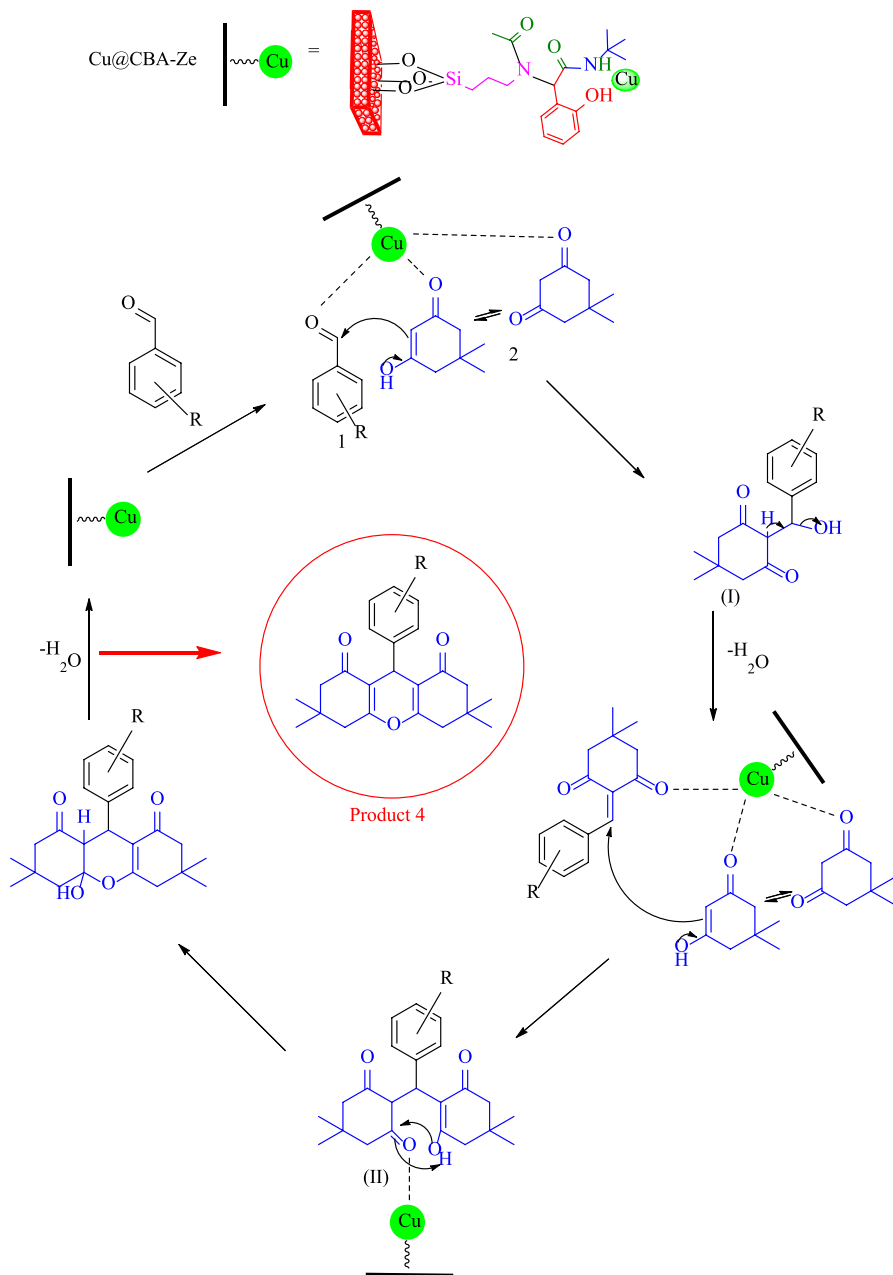
**Scheme 3** A suggested mechanism for the synthesis of compounds **4**

Recovering and reusing catalysts in chemical processes is always a challenge. Specifically, this context examines how well the catalysts used in the model reaction can be recovered, reused, and leached. The Cu@CBA-Ze heterogeneous catalyst
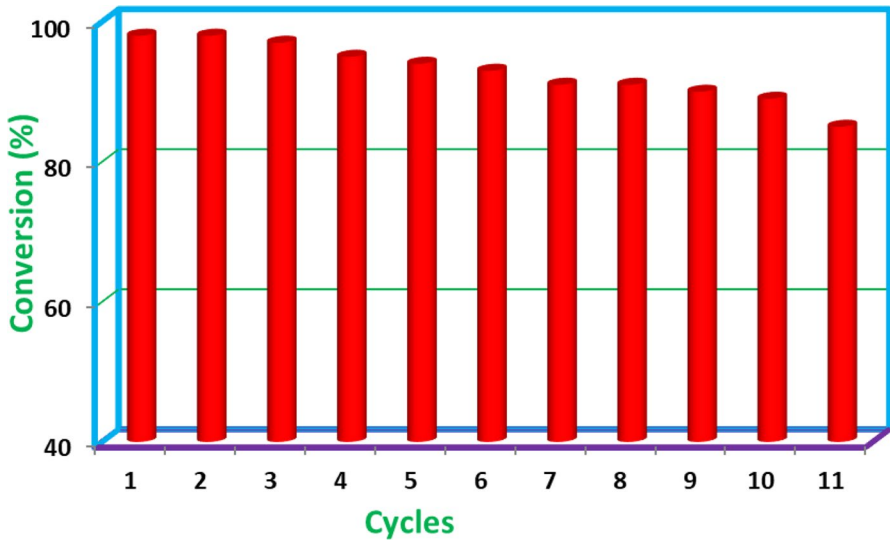
Fig. 11 Reusability of catalyst in the model reaction

showed the potential to be an effective solid catalyst for the preparation of xanthenes by filtration and reused for at least eleven cycles (Fig. 11).

After eleven successive cycles of Cu@CBA-Ze reuse, the SEM and TEM images as well as the XRD patterns and the FT-IR spectrum show no significant differences from fresh Cu@CBA-Ze images and catalyst properties and activity have remained unchanged (Fig. 12).
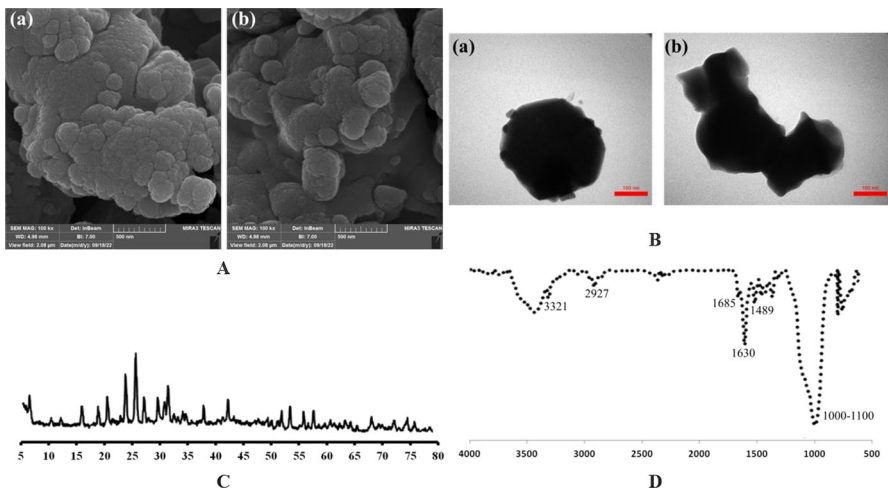
Fig. 12 A SEM images of (**a**): fresh NaY-Ugi and (**b**): reused Cu@CBA-Ze after eleven cycles (**B**): TEM images of (**a**): fresh NaY-Ugi and (**b**): reused Cu@CBA-Ze after eleven cycles (**C**): XRD patterns of the reused Cu@CBA-Ze after eleven cycles (**D**): IR spectra of the reused Cu@CBA-Ze after eleven cycles

Test of synthesized catalyst leaching has been investigated on the model reaction under general conditions. Although the reaction was supposed to be completed in 30 min, it was stopped after 15 min to collect the catalyst through centrifugation. A GC analysis was performed to measure the reaction yield (81%). A 30-min stirring of the reaction mixture without a catalyst did not change the product yield as calculated again by GC. The results indicate that there is no catalyst leaching after the reaction is complete.

Conclusion

This study describes the simple and direct synthesis of carboxamide-functionalized nano NaY zeolite (CBA-Ze) to obtain a new high-functionality catalytic system in one pot process. This surface modification was achieved using a Ugi four-component reaction, followed by immobilization of copper ions on the Ugi-ligands decorated nano NaY zeolite surface. The synthesized catalysts were characterized using techniques such as FT-IR, TGA, DTA, SEM, TEM, XRD, DLS, EDS, ICP, and elemental analyses. The nature of the bonded Ugi-ligand on the zeolite's surface improved the catalyst reactivity, and homogeneity and increased its capability to coordinate with copper ions. The catalyst efficiency of the synthesized copper-carboxamide complex immobilized on nano NaY zeolite (Cu@CBA-Ze) was investigated in the synthesis of Xanthens, leading to product yields of 85–98% in H_2O: EtOH (1:1) at room temperature within 30 min. Ease of catalyst recovery, simple setup procedure, high stability, simple work-up, short reaction time, excellent product yields, and reusability of catalyst for eleven consecutive runs are the significant advantages of the presented work. This study introduces a catalytic system that can potentially produce other beneficial heterocyclic compounds under mild environmental conditions.

Experimental

Materials

Merck Company supplied (3-aminopropyl)triethoxysilane (APTES), 2-hydroxyben-zaldehyde, tert-butyl isocyanide, glacial acetic acid, copper (II) acetate, and solvents (Germany). NaY nanozeolite (Si/Al = 2.5) was provided by Zeolyst corporation (USA).

Physicochemical techniques

Melting points were measured using the Electrothermal IA9100 (Essex, UK). A Bruker Avance DRX-400 NMR spectrometer (Bruker, Germany) recorded ^{1}H and ^{13}C NMR spectra with TMS as internal reference and $CDCl_3$ as solvent. The synthesized samples were identified by applying X-ray powder diffraction (Philips

PW-1830), TGA apparatus (Netzsch, Selb, Germany), FT-IR spectrometers (Bruker Tensor 27, Germany), dynamic light scattering (DLS) on (HORIBA SZ-100, Ltd., Japan), and scanning electron microscopy (SEM) (Tescan, Brno, Czech Republic).

Synthesis of catalyst

General synthesis of APTES-modified nanozeolites (AP-Ze)

To a mixture of 1.00 g of NaY nanozeolite (Ze) in dry toluene (30 mL), 2.33 mL of APTES (10.0 mmol) was added under a nitrogen atmosphere and refluxed for 8 h. To collect the APTES-modified nanozeolites (AP-Ze), the mixture was centrifuged after cooling to room temperature. Unreacted APTES was removed using a Soxhlet extractor with 150 mL 99.5% ethanol for 24 h [4].

General synthesis for producing carboxamide-functionalized nanozeolite (CBA-Ze)

Carboxamide-functionalized nanozeolite (CBA-Ze) was prepared according to reported procedures [4, 6]. To a solution of 2-hydroxybenzaldehyde (5.00 mmol, 0.52 mL) in EtOH (25 mL), NaY-AP (0.50 g) was added and allowed to be stirred for 30 min at ambient temperature. Then tert-butylisocyanide (5.00 mmol, 0.56 mL) and glacial acetic acid (5.00 mmol, 0.28 mL) were added to the mixture and stirred at ambient temperature for 12 h. After cooling to room temperature, the carboxa-mide-functionalized nanozeolite (CBA-Ze) was purified by washing with Ethanol/Acetone and separated using centrifugation (8000 rpm, 10 min, 5 times).

General procedure for preparation of Cu@CBA-Ze (Cu@CBA-Ze)

1.00 g of CBA-Ze was dispersed in water and ultrasonicated at room temperature. Then, copper (II) acetate (0.09 g, 0.50 mmol in 10 mL H_2O) was added dropwise to the reaction mixture. The reaction mixture was stirred over 24 h at 80 °C. The Cu@CBA-Ze were centrifuged and washed three times with deionized water (8000 rpm, 5 min, 3 times) [6].

Synthesis of xanthenes

General procedure for the synthesis of xanthenes

A mixture of aromatic aldehyde (1 mmol), dimedone (2 mmol), and/or β-naphthol (2 mmol), Cu@CBA-Ze catalyst (20 mg) in H_2O: EtOH (1:1) (10 mL) was stirred at room temperature for 30 min. After reaction completion (checked by TLC, n-Hex-ane: EtOAc (3:1) as eluent), the catalyst was separated through centrifugation. The
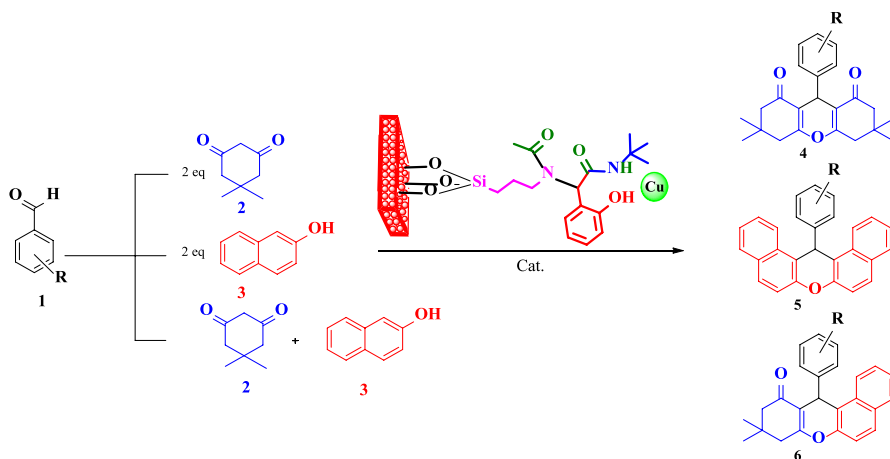
Scheme 4 Synthesis of xanthenes using Cu@CBA-Ze

solvent was removed under reduced pressure and the solid product recrystallized from ethanol (Scheme 4).

Spectral data for selected samples (4a, 5a, 6a, 4d, 5d, and 6c)

9-(4-chlorophenyl)-3,3,6,6-tetramethyl-3,4,5,6,7,9-hexahydro-1*H*-x anthene-1,8(2*H*)-dione (4a)

Light yellow powder, m.p. 204–205 °C, yield: 94%; ^{1}H NMR (CDCl$_3$, 400 MHz): δ 1.01 (s, 6H, 2CH$_3$), 1.12 (s, 6H, 2CH$_3$), 2.19 and 2.25 (ABq, 4H, $J = 16.0$ Hz, 2CH$_2$), 2.48 (s, 4H, 2CH$_2$), 4.73 (s, 1H, CH), 7.19–7.26 (m, 4H, CH$_{Ar}$). ^{13}C NMR (CDCl$_3$, 100 MHz): δ 27.2, 29.2, 31.4, 32.2, 40.8, 50.6, 115.2, 128.2, 129.7, 132.0, 142.6, 162.4, 196.3.

14-(4-chlorophenyl)-14*H*-dibenzo[*a,j*]xanthene (5a)

Pink powder, m.p. 182–184 °C, yield: 91%; ^{1}H NMR (CDCl$_3$, 400 MHz): δ 6.49 (s, 1H, CH), 7.12 (d, 2H, $J = 8.0$ Hz, CH$_{Ar}$), 7.42–7.51 (m, 6H, CH$_{Ar}$), 7.58–7.62 (m, 2H, CH$_{Ar}$), 7.83 (d, 2H, $J = 8.0$ Hz, CH$_{Ar}$), 8.56 (d, 2H, $J = 8.0$ Hz, CH$_{Ar}$), 8.34 (d, 2H, $J = 8.0$ Hz, CH$_{Ar}$). ^{13}C NMR (CDCl$_3$, 100 MHz): δ 37.3, 116.7, 118.0, 122.4, 124.3, 126.9, 128.6, 128.9, 129.0, 129.4, 131.0, 131.2, 132.0, 143.4, 148.6.

12-(4-chlorophenyl)-9,9-dimethyl-9,10-dihydro-8*H*-benzo[a]xanthen-11(12*H*)-one (6a)

Light yellow powder, m.p. 176–177 °C, yield: 94%; ^{1}H NMR (CDCl$_3$, 400 MHz): δ 0.98 (s, 3H, CH$_3$), 1.14 (s, 3H, CH$_3$), 2.27 and 2.33 (ABq, 2H, $J = 16.0$ Hz, CH$_2$), 2.59 (s, 2H, CH$_2$), 5.70 (s, 1H, CH), 7.14–7.17 (m, 2H, CH$_{Ar}$), 7.28–7.31 (m, 2H, CH$_{Ar}$), 7.34 (d, 1H, $J = 8.0$ Hz, CH$_{Ar}$), 7.39–7.43 (m, 1H, CH$_{Ar}$), 7.44–7.48 (m, 1H, CH$_{Ar}$), 7.78–7.82 (m, 2H, CH$_{Ar}$), 7.92 (d, 1H, $J = 8.0$ Hz). ^{13}C NMR (CDCl$_3$, 100 MHz): δ 27.1, 29.3, 32.2, 34.1, 41.4, 50.8, 113.8, 117.0, 123.4, 125.0, 127.1, 128.3, 128.4, 1285, 129.1, 129.8, 131.2, 131.5, 131.9, 143.2, 147.7, 164.0, 196.9.

6-tetramethyl-9-(4-nitrophenyl)-3,4,5,6,7,9-hexahydro-1*H*-xanthene-1,8(2*H*)-dione (4d)

Light yellow powder, m.p. 230–232 °C, yield: 97%; ^{1}H NMR (CDCl$_3$, 400 MHz): δ 1.00 (s, 6H, 2CH$_3$), 1.14 (s, 6H, 2CH$_3$), 2.16 and 2.29 (ABq, 4H, $J = 16.00$ Hz, 2CH$_2$), 2.51 (s, 4H, 2CH$_2$), 4.84 (s, 1H, CH), 7.49 (d, 2H, $J = 8$ Hz, CH$_{Ar}$), 8.11 (d, 2H, $J = 8$ Hz, CH$_{Ar}$). ^{13}C NMR (CDCl$_3$, 100 MHz): δ 27.2, 29.2, 32.2, 32.5, 40.8, 50.5, 110.2, 114.5, 123.4, 129.3, 146.4, 151.5, 162.9, 196.2.

14-(4-nitrophenyl)-14*H*-dibenzo[*a,j*]xanthene (5d)

Brown powder, m.p. 316–318 °C, yield: 94%; ^{1}H NMR (CDCl$_3$, 400 MHz): δ 6.62 (s, 1H, CH), 7.44– 7.48 (m, 2H, CH$_{Ar}$), 7.53 (d, 2H, $J = 8$ Hz, CH$_{Ar}$), 7.60–7.64 (m, 2H, CH$_{Ar}$), 7.69 (d, 2H, $J = 8$ Hz, CH$_{Ar}$), 7.84–7.88 (m, 2H, CH$_{Ar}$), 8.02 (d, 2H, $J = 8$ Hz, CH$_{Ar}$), 8.30 (d, 2H, $J = 8$ Hz, CH$_{Ar}$). ^{13}C NMR (CDCl$_3$, 100 MHz): δ 37.8, 115.7, 118.0, 122.0, 123.8, 124.5, 127.1, 128.9, 129.0, 129.5, 131.0, 131.1, 146.2, 148.7, 152.0.

9-dimethyl-12-(4-nitrophenyl)-9,10-dihydro-8*H*-benzo[a]xanthen-11(12*H*)-one (6c)

Yellow powder, m.p. 173–174 °C, yield: 98%; ^{1}H NMR (CDCl$_3$, 400 MHz): δ 0.97 (s, 3H, CH$_3$), 1.16 (s, 3H, CH$_3$), 2.25 and 2.38 (ABq, 2H, $J = 16.00$ Hz, CH$_2$), 2.62 (s, 2H, CH$_2$), 5.84 (s, 1H, CH), 7.38 (d, 1H, $J = 8$ Hz, CH$_{Ar}$), 7.40–7.48 (m, 2H, CH$_{Ar}$), 7.54 (d, 2H, $J = 8$ Hz, CH$_{Ar}$), 7.81–7.86 (m, 3H, CH$_{Ar}$), 8.05 (d, 2H, $J = 8$ Hz, CH$_{Ar}$). ^{13}C NMR (CDCl$_3$, 100 MHz): δ 27.0, 29.3, 32.2, 34.9, 41.4, 50.7, 112.9, 116.0, 117.1, 123.1, 123.6, 125.2, 127.3, 128.6, 129.3, 129.6, 131.0, 131.5, 146.3, 151.8, 164.6, 196.7.

Author contributions All persons who meet authorship criteria are listed as follows, and all authors certify that they have participated sufficiently in the work to take public responsibility for the content, including participation in the concept, design, analysis, writing, or revision of the manuscript.

Declarations

Conflict of interest It is to specifically state that "No Competing interests are at stake and there is No Conflict of Interest" with other people or organizations that could inappropriately influence or bias the content of the paper.

Ethical approval Not applicable.

Consent to participate Not applicable.

Consent for publication Not applicable.

References

1. S. Montalvo, L. Guerrero, R. Borja, E. Sánchez, Z. Milán, I. Cortés, M.A. De La La Rubia, Appl. Clay Sci. **58**, 125 (2012)
2. F. Babaei, S. Asghari, M. Tajbakhsh, Res. Chem. Intermed. **45**, 4693 (2019)
3. M. Azizi Amiri, G.F. Pasha, M. Tajbakhsh, S. Asghari, Appl. Organomet. Chem. **36**, 6886 (2022)
4. H. Younesi, S. Asghari, G.F. Pasha, M. Tajbakhsh, Appl. Organomet. Chem. **37**, 7127 (2023)
5. R. Razavian Mofrad, H. Kabirifard, M. Tajbakhsh, G.F. Pasha, Appl. Organomet. Chem. **35**, 6383 (2021)
6. A. Shaabani, R. Afshari, J. Colloid Interface Sci. **510**, 384 (2018)
7. A. Dömling, Curr. Opin. Chem. Biol. **4**, 318 (2000)
8. A. Shaabani, S.E. Hooshmand, RSC Adv. **6**, 58142 (2016)
9. I. Ugi, Pure Appl. Chem. **73**, 187 (2001)
10. C. Hebach, U. Kazmaier, Chem. Commun. **5**, 596 (2003)
11. G. Koopmanschap, E. Ruijter, R.V. Orru, Beilstein J. Org. Chem. **10**, 544 (2014)
12. S.L. Jain, P. Bhattacharyya, H.L. Milton, A.M. Slawin, J.A. Crayston, J.D. Woollins, Dalton Trans. **6**, 862 (2004)
13. A. Rezaei, O. Akhavan, E. Hashemi, M. Shamsara, Biomacromol **17**, 2963 (2016)
14. A. Shaabani, R. Afshari, ChemistrySelect **2**, 5218 (2017)
15. S. Kamino, M. Uchiyama, Org. Biomol. Chem. **21**, 2458 (2023)
16. A.M. Abdelghany, A.A. Menazea, M.A. Abd-El-Maksoud, T.K. Khatab, Appl. Organomet. Chem. **34**, 5250 (2020)
17. C.G. Knight, T. Stephens, Biochem. J. **258**, 683 (1989)
18. S.M. Amininasab, E. Ghoseiri, S. Abdolmaleki, Macromol. Res. **30**, 891 (2022)
19. H.N. Hafez, M.I. Hegab, I.S. Ahmed-Farag, A.B.A. El-Gazzar, Bioorg. Med. Chem. Lett. **18**, 4538 (2008)
20. S.J. Santos, F.C. Rossatto, N.S. Jardim, D.S. Ávila, R. Ligabue-Braun, L.A. Fontoura, D. Russowsky, New J. Chem. **47**, 7500 (2023)
21. T.S. Jin, L.B. Liu, Y. Zhao, T.S. Li, Synth. Commun. **35**, 2379 (2005)
22. R. Jesu-Jaya-Sudan, J. Lesitha-Jeeva-Kumari, P. Iniyavan, S. Sarveswari, V. Vijayakumar, Mol. Divers **27**, 709 (2023)
23. A.H. Bedair, N.A. El-Hady, M.S.A. El-Latif, A.H. Fakery, A.M. El-Agrody, Farmaco **55**, 708 (2000)
24. S. Abdolmohammadi, Z. Hossaini, Z. Azizi, ChemistrySelect **8**, 202300343 (2023)
25. L. Applová, E. Veljovic, S. Muratovic, J. Karlickova, K. Macakova, D. Zavrsnik, P. Mladenka, Med. Chem. **14**, 200 (2018)

26. F. Chabchoub, M. Messaâd, H. Ben-Mansour, L. Ghdira, M. Salem, Eur. J. Med. Chem. **42**, 715 (2007)
27. O. Bruno, C. Brullo, S. Schenone, A. Ranise, F. Bondavalli, E. Barocelli, M. Tognolini, F. Magnanini, V. Ballabeni, Farmaco **57**, 753 (2002)
28. U.I. Kasabe, K.B. Kale, N.R. Rode, A.V. Shelar, R.H. Patil, P.C. Mhaske, M.G. Chaskar, New J. Chem. **46**, 2128 (2022)
29. M. Messaâd, F. Chabchoub, M. Salem, Heterocycl. Commun. **9**, 401 (2005)
30. S. Kantevari, R. Bantu, L. Nagarapu, J. Mol. Catal. A Chem. **269**, 53 (2007)
31. S. Mondal, A.M. Pandey, B. Gnanaprakasam, React. Chem. Eng. **8**, 855 (2023)
32. B. Das, B. Ravikanth, R. Ramu, K. Laxminarayana, B.V. Rao, J. Mol. Catal. A: Chem. **255**, 74 (2006)
33. E. Pourian, S. Javanshir, Z. Dolatkhah, S. Molaei, A. Maleki, ACS Omega **3**, 5012 (2018)
34. S.M. Mousavifar, H. Kefayati, S. Shariati, Appl. Organomet. Chem. **32**, 4242 (2018)
35. Subodh, N.K. Mogha, K. Chaudhary, G. Kumar, D.T. Masram, ACS Omega **3**, 16377 (2018)
36. L. Moradi, M. Mirzaei, RSC Adv. **9**, 19940 (2019)
37. S. Naderi, R. Sandaroos, S. Peiman, B. Maleki, J. Phys. Chem. Solids **180**, 111459 (2023)
38. F. Moradi, M. Abdoli-Senejani, React. Kinet. Mech. Catal. **136**, 1357 (2023)
39. A. Alipour, H. Naeimi, Res. Chem. Intermed. **49**, 2705 (2023)
40. M.M. Zeydi, Russ. J. Org. Chem. **58**, 557 (2022)
41. S.M. Baghbanian, G. Khanzad, S.M. Vahdat, H. Tashakkorian, Res. Chem. Intermed. **41**, 9951 (2015)
42. K. Gong, D. Fang, H.L. Wang, X.-L. Zhou, Z.L. Liu, Dyes Pigm. **80**, 30 (2009)
43. A. Zhu, S. Bai, W. Jin, R. Liu, L. Li, Y. Zhao, J. Wang, RSC Adv. **4**, 36031 (2014)
44. S.M. El-Dafrawy, R.S. Salama, S.A. El-Hakam, S.E. Samra, J. Mater. Res. **9**, 1998 (2020)
45. K. Tabatabaeian, M.A. Zanjanchi, M. Mamaghani, A. Dadashi, Can. J. Chem. **92**, 1086 (2014)
46. A. Rezaei, O. Akhavan, E. Hashemi, M. Shamsara, Chem. Mater. **28**, 3004 (2016)
47. O.S. Travkina, M.R. Agliullin, N.A. Filippova, A.N. Khazipova, I.G. Danilova, N.N.G. Grigor'Eva, B.I. Kutepov, RSC Adv. **7**, 32581 (2017)
48. K. Sivakumar, A. Santhanam, M. Natarajan, D. Velauthapillai, B. Rangasamy, Int. J. Appl. Ceram. Technol. **13**, 1182 (2016)
49. W. Rongchapo, C. Keawkumay, N. Osakoo, K. Deekamwong, N. Chanlek, S. Prayoonpokarach, J. Wittayakun, Adsorpt. Sci. Technol. **36**, 684 (2018)
50. P.S. Bhale, S.B. Dongare, Y.B. Mule, Chem. Sci. Trans. **4**, 246 (2015)
51. Z. Zhou, X. Deng, J. Mol. Catal. A Chem. **367**, 99 (2013)
52. K. Kundu, S.K. Nayak, J. Serb. Chem. Soc. **79**, 1051 (2014)
53. D.S. Rekunge, C.K. Khatri, G.U. Chaturbhuj, Monatsh. Chem. **148**, 2091 (2017)
54. Y. Cao, C. Yao, B. Qin, H. Zhang, Res. Chem. Intermed. **39**, 3055 (2013)
55. R. Mohammadi, E. Eidi, M. Ghavami, M.Z. Kassaee, J. Mol. Catal. A Chem. **393**, 309 (2014)
56. S. Ghassamipour, R. Ghashghaei, Monatsh. Chem. **146**, 159 (2015)
57. K. Niknam, F. Panahi, D. Saberi, M. Mohagheghnejad, J. Heterocycl. Chem. **47**, 292 (2010)
58. G. Song, B. Wang, H. Luo, L. Yang, Catal. Commun. **8**, 673 (2007)
59. M.T. Maghsoodlou, S.M. Habibi-Khorassani, Z. Shahkarami, N. Maleki, M. Rostamizadeh, Chin. Chem. Lett. **21**, 686 (2010)
60. A. Ilangovan, S. Muralidharan, P. Sakthivel, S. Malayappasamy, S. Karuppusamy, M.P. Kaushik, Tetrahedron Lett. **54**, 491 (2013)
61. K. Niknam, M. Damya, J. Chin. Chem. Soc. **56**, 659 (2009)
62. S. Rezayati, R. Hajinasiri, Z. Erfani, S. Rezayati, S. Afsharisharifabad, Iran. J. Catal. **4**, 157 (2014)
63. G.R. Chaudhary, P. Bansal, N. Kaur, S.K. Mehta, RSC Adv. **4**, 49462 (2014)
64. A.N. Dadhania, V.K. Patel, D.K. Raval, J. Saudi Chem. Soc. **21**, 163 (2017)